DESIGN AND DEVELOPMENT OF A NiTiNOL ACTUATED, CRAB-LIKE MILLISCALE OCTABOT

D. Rashmi[a], Anoop Singh Yadav[b], Sunilkumar Ainwad[c]

[a]Scientist, DRDO Young Scientists' Laboratory for Smart Materials, Hyderabad, India
[b]Junior Research Fellow, DRDO Young Scientists' Laboratory for Smart Materials, Hyderabad, India
[c]Project Engineer, DRDO Young Scientists' Laboratory for Smart Materials, Hyderabad, India

Abstract. This paper introduces a novel design for a centimetre-scale side-crawling 'Octabot' robot inspired by crab locomotion. The robot imitates the crab's ability to crawl in two directions through the adduction and abduction of its legs, making this feature unique to the design. The prototype has been fabricated through Smart Composite Microstructure technique. NiTiNOL wire has been used for actuation considering the advantage it offers in terms of power density, given the size constraint. Inverse and forward kinematics have been implemented to calculate the joint angles and leg trajectory, attributed to a 4% strain in the NiTiNOL wire. Control signals are pulsed at timed intervals to channels on either side for sequential adduction and abduction of legs. The Octabot has demonstrated a crawling speed of 2.5 mm/s.

Keywords: Bioinspired robot, Crab-like, NiTiNOL, Kinematics

1 Introduction

Milli-scale autonomous robots embedded with sensor arrays prove to be extremely advantageous in surveillance of hazardous environments. This demand has led to a surged interest in the area of milli-scale legged robots. Crabs are recognized for their distinct sideways movement at remarkable speeds, yet they have not been extensively studied in the field of robotics. Investigating the locomotion of these side-walking creatures presents an interesting area of research in legged millirobotics. A study conducted by Chen et al [1] reported that the sideways walking motion of a robot resembling a crab is found to be more efficient when compared to its forward walking motion in terms of speed and cost of transport.

Several attempts have been made at the design of insect-scale millirobots actuated through NiTiNOL. Baisch et al [2] utilized Smart Composite Microstructure (SCM) technique to create a 90 mg microrobot with a hexapedal structure. This tiny robot has 8 degrees of freedom (DoF) and operates using an alternating tripod gait. The microrobot incorporates both proximal and distal NiTiNOL springs for its movement, enabling it to crawl at frequencies of 1/3 Hz and 1 Hz. The research findings indicate that increasing the actuation speed results in reduced leg displacement, and the microrobot is also capable of executing a zero-radius turn. Hoover et al [3] designed a cockroach-inspired millirobot exhibiting 2 DoF including leg adduction and abduction as well as extension and flexion, operating at 3Hz. Multi-material 3D printing of a combination of soft elastic and rigid materials for prototyping of milli/micro scale robotics has been very successful in mimicking the stiffness variations present in the anatomy of natural organisms, thus attempting to impart animal-like mobility [4].

The present paper attempts to extend the ongoing research towards the development of a crab-like Octabot capable of a sideways crawl through sequential actuation of adducting and abducting legs. The robot has been fabricated out of carbon-fiber/epoxy composite using SCM technique to provide flexure hinges for generating the above movement pattern. NiTiNOL wire routed along the legs is controlled through two channels for each side movement. Inverse kinematics (IK) to obtain the deflected leg joint angles has been carried out for a given point whose coordinates have been obtained through a prescribed strain in the NiTiNOL wire. The leg trajectories have been obtained through forward kinematic (FK) analysis. The locomotive capabilities of the Octabot have been tested and demonstrated in the present work.

2 Design

2.1 Mechanical design

Crabs are decapods that employ eight of their appendages for surface locomotion. In the present paper, to mimic the terrestrial locomotion of crabs, an Octabot is designed with eight legs that are sequentially moved in the mid-sagittal plane through adduction and abduction. Two DoF been incorporated into each leg with the help of the coxa-merus and merus-propus joints, as depicted in Fig.1. Additionally, the abducting legs have been equipped with an additional dactylus feature that is angled inwards to ensure proper contact with the ground during movement.

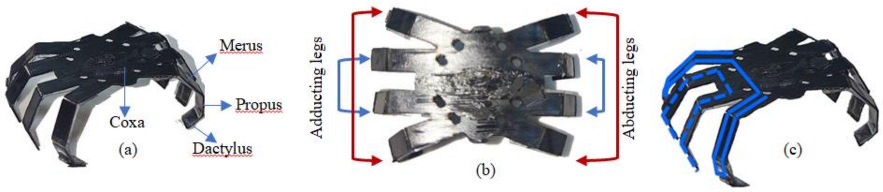

Fig. 1. (a) Design features of Octabot (b) Indication of leg functionality (c) NiTiNOL routing on abducting and adducting legs

The dimensions of the Octabot are 20×35×15 mm. The weight of the untethered prototype, including NiTiNOL, electrical contact wire, solder, and crimps, is 1.45 grams. The design of the Octabot includes eight legs, with the middle four legs capable of adducting (moving towards the center) and the outer four legs capable of abducting (moving away from the center). The angle of merus, propus, and dactylus with respect to coxa is obtained through the IK analysis for a given point in the workspace.

2.2 Fabrication

Fabrication of the prototype is carried out through SCM technique due to its simplicity and effectiveness in facilitating flexure joints between rigid links [5]. Two sheets of carbon-fiber prepreg of 150 µm thickness are marked with dimensions (40×0.1 mm) of the flexure hinges that are to be cut out. A polyester tape of 150 µm thickness is sandwiched between two such replica-cut carbon sheets. The composite is compacted in a mold at 125°C for 2 hours to cure before undergoing a final round of laser cuts to obtain the desired shape and size as shown in Fig.2(a) after cooling composite. To enhance the bending stiffness at the joint, a layer of 250 µm thick polyethylene terephthalate (PET) is been glued underneath the hinges, as illustrated in Fig.2(b). The 2D layup is bent at desired angles to form the 3D structure of the leg illustrated in Fig2(c). The rigidity of the PET layer helps in maintaining the leg angle while supporting the overall weight of the Octabot.

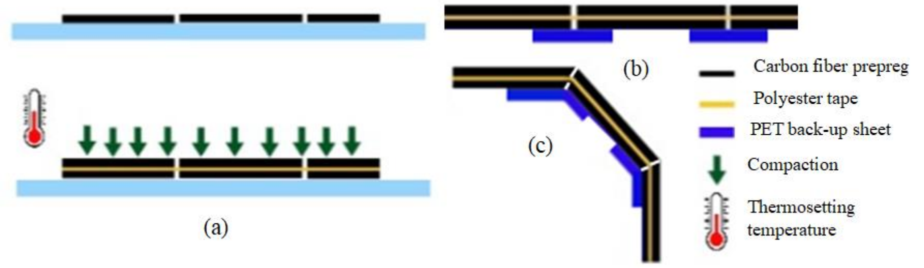

Fig. 2. (a) Smart Composite Microstructure fabrication process (b) Cured 2D specimen with PET back-up sheet (c) Propped 3D specimen with 2R flexure hinges

2.3 Actuation

NiTiNOL wire has been routed through the flexure hinges for joint articulation. When heated beyond the transformation temperature, NiTiNOL experiences a phase transition from daughter phase (martensite) to parent phase (austenite) while experiencing a contractile strain of ~4%. A ϕ 0.1mm NiTiNOL wire (Flexinol®, Dynalloy Inc) is chosen considering the essential factors of force, power, and operating frequency required for the desired actuation. The austenitic start (As) and finish (Af) temperatures of NiTiNOL wire is 88°C and 98°C [6]. As illustrated in Fig.1(c), the NiTiNOL wire has been routed underneath from the propus of the adducting leg to the coxa, causing the leg to bend inwards, upon actuation. On the abducting legs, the NiTiNOL wire has been routed along the upper surface of the legs, passing through the propus-merus, and then crimped at the coxa, causing it to expand outwards.

A sequentially coupled joule heating and transient thermal analysis has been carried out using COMSOL Multiphysics® to identify the optimum current pulse parameters required to heat the NiTiNOL wire to its transformation temperature while avoiding over-heating. This study is critical in deciding the time period of the actuation cycle to achieve a desired crawling speed. If the gait cycle involves a hold-time between the stance and swing phases, a minimum current required to hold the wire temperature for the intended time is identified, as shown in Fig.3.

During actuation tests, in-situ measurements of wire temperature through contact (thermocouple) and non-contact (infrared detector/camera) methods were unable to capture the real-time high-speed thermal transients due to low response time and thin profile (low Biot number) of the wire. The thermal analysis model has been validated through video-recording of the actuation experiments and noting the time instants during the onset and end of transformation. For the validation experiment, NiTiNOL wire of the same diameter that has been shape trained to a spring is stretched back to a wire before actuation. The wire recovers the trained spring shape upon the application of current pulse depicted in Fig.3. The video frames pertaining to the onset and end of transformation have been extracted and the time instants noted. The transformation finish time can be confirmed from the complete recovery of the trained spring shape of the wire. These time instants correspond to A_s and A_f occurring at 0.4s and 0.7s respectively. The temperatures at these time instants extracted from the model are 86.35°C and 99.25°C that matches closely with the values mentioned in the NiTiNOL data sheet. The results are plotted in Fig.4.

The Fig.5'

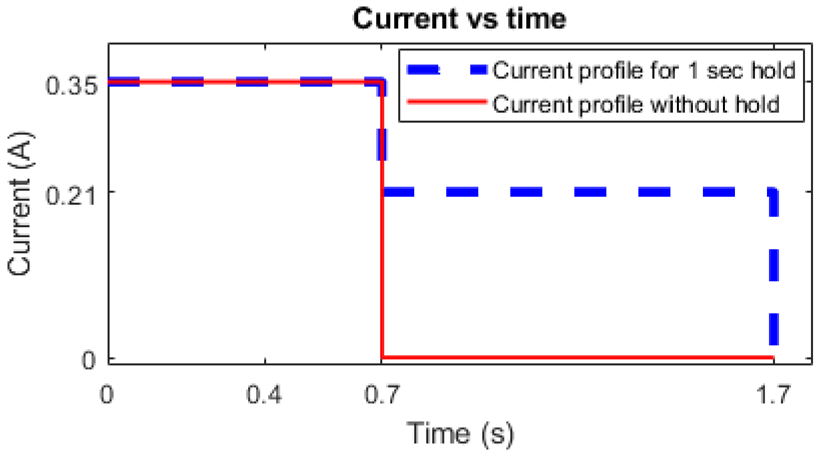

Fig. 3. Plots of Supplied electric current vs time

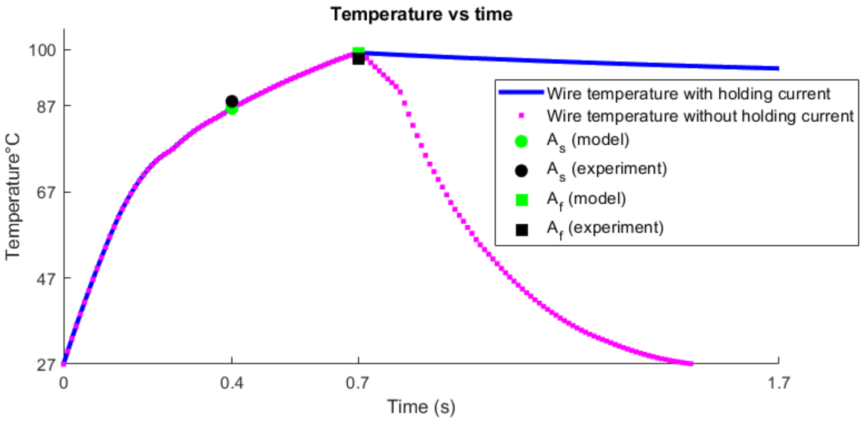

Fig. 4. Plot of temperature vs time

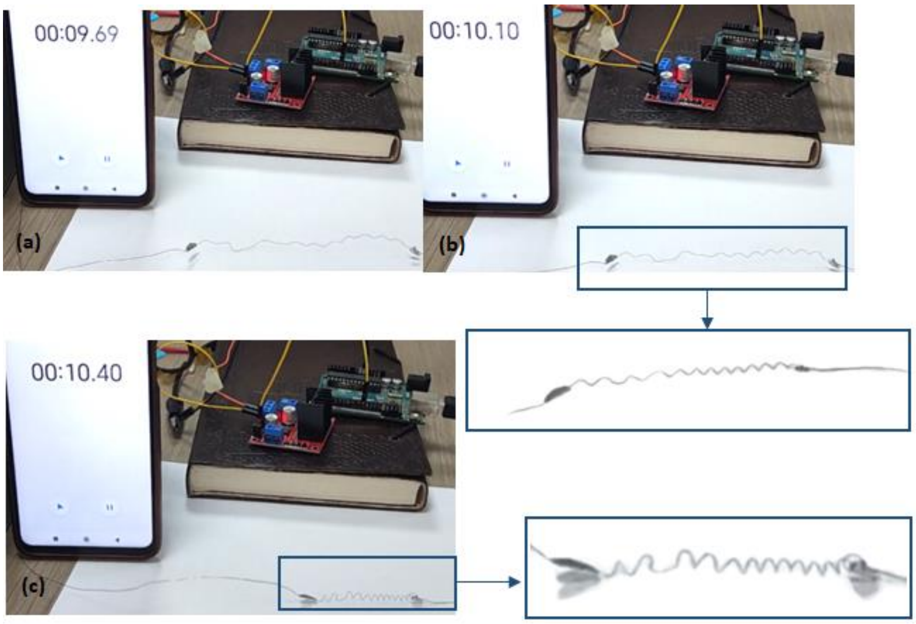

Fig. 5. Plots for validation of numerical study (a) At time t=0, initiate the heating of deformed NiTiNOL spring (b) At time t=0.4, NiTiNOL spring achieved the A_s temperature (c) At time t=0.7, NiTiNOL spring achieved the A_f temperature

3 Kinematics

The standard approach for modelling the kinematics of flexure hinges is through large deformation pseudo-rigid body modelling [7, 8, 9]. In the present scope, given the robot size and limited strain of NiTiNOL, a rigid body approach serves as a good approximation. The adducting and abducting legs are idealized as 2R and 3R revolute joints, as shown in Fig.6.

The links of lengths l_1, l_2 and l_3 have been modelled as mobile links representing the merus, propus and dactylus respectively while link of length l_0 representing the coxa is fixed. The workspace of these configurations is a circle of radius equal to the lengths of the links. The initial joint angles (θ_1^i, θ_2^i) at which the PET layer is bent have been calculated through IK based on a chosen point in the workspace i.e. (x_2, y_2) for 2R joint and (x_3, y_3) for 3R joint. Newton-Raphson method is employed for IK with the criterion for absolute error set to $\leq 10^{-5}$.

The dactylus angle θ_3 is fixed at 86° to obtain a large horizontal movement and thus ensuring ground contact during actuation. NiTiNOL wire initially offers 5-8% strain for a limited number of cycles, followed by 3-5% strain for millions of cycles [6]. A strain of 4% corresponding to NiTiNOL actuation has been considered for analysis. The direction of the resultant strain is obtained from the wire route. The horizontal and vertical components of the resultant have been used to calculate the final tip coordinates. Based on the final tip coordinates, the final joint angles (θ_1^f, θ_2^f) have been calculated using IK. The trajectory of the leg tip is calculated through FK calculations as listed in equations 1-6, incrementing the joint angles from θ_i to θ_f. The procedure has been illustrated in the form of a flowchart in Fig.7. The algorithms for FK and IK have been implemented in MATLAB. The results of the analysis are discussed in detail in Section 5.

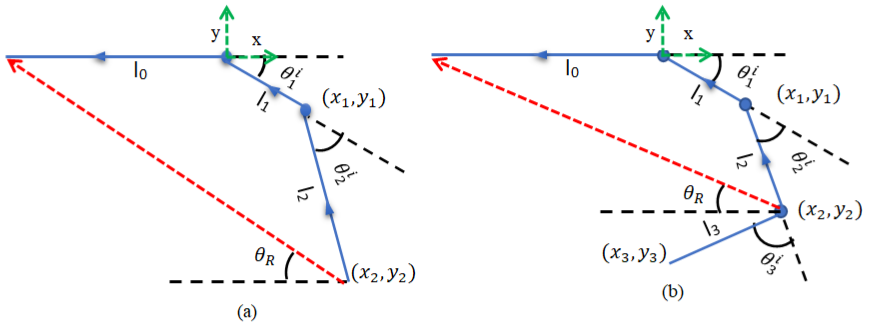

Fig. 6. Rigid body diagrams for (a) adducting leg (2R) (b) abducting leg (3R)

The coordinates of links l_1, l_2 that are common to both 2R adducting and 3R abducting legs can be obtained through the following relations.

$$x_1 = l_0 + l_1 \cos\theta_1 \tag{1}$$

$$y_1 = l_1 \sin\theta_1 \quad (2)$$

$$x_2 = l_0 + l_1 \cos\theta_1 + l_2 \cos(\theta_1 + \theta_2) \quad (3)$$

$$y_2 = l_1 \sin\theta_1 + l_2 \sin(\theta_1 + \theta_2) \quad (4)$$

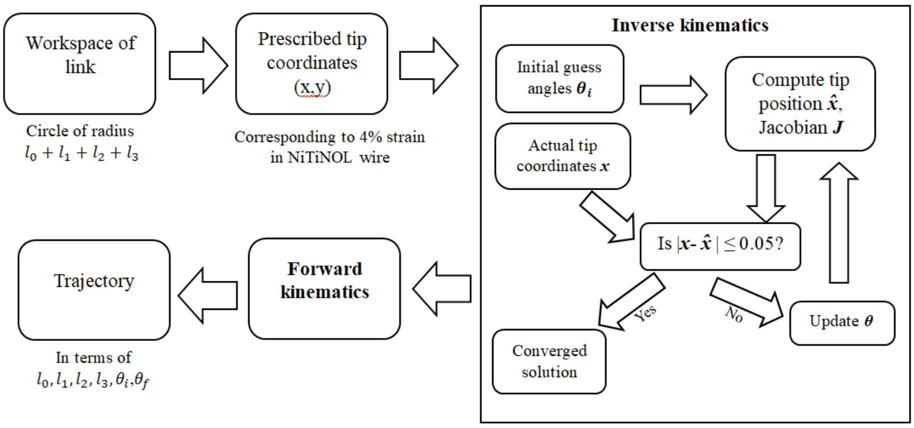
Workspace of link
Circle of radius $l_0 + l_1 + l_2 + l_3$
Prescribed tip coordinates (x,y)
Corresponding to 4% strain in NiTiNOL wire
Inverse kinematics
Initial guess angles $\boldsymbol{\theta}_i$
Compute tip position $\hat{\boldsymbol{x}}$, Jacobian $\boldsymbol{J}$
Actual tip coordinates $\boldsymbol{x}$
Is $|\boldsymbol{x}-\hat{\boldsymbol{x}}| \le 0.05$?
Yes
No
Update $\boldsymbol{\theta}$
Converged solution
Forward kinematics
Trajectory
In terms of $l_0, l_1, l_2, l_3, \theta_i, \theta_f$

Fig. 7. Flow chart of kinematic analysis

The coordinates of the additional link l_3 present in the 3R abducting leg can be obtained by the following equations.

$$x_3 = l_0 + l_1 \cos\theta_1 + l_2 \cos(\theta_1 + \theta_2) + l_3 \cos(\theta_1 + \theta_2 + \theta_3) \quad (5)$$

$$y_3 = l_1 \sin\theta_1 + l_2 \sin(\theta_1 + \theta_2) + l_3 \sin(\theta_1 + \theta_2 + \theta_3) \quad (6)$$

Table 1. Inverse Kinematic Calculations to calculate initial angles θ_i

Adducting leg (2R)	Abducting leg (3R)
Desired tip coordinates $\boldsymbol{x}$, (x_2, y_2) = (5.45, -8.70)	Desired tip coordinates $\boldsymbol{x}$, (x_3, y_3) = (0.70, -8.70)
	Desired tip coordinates $\boldsymbol{x}$, (x_2, y_2) = (5.39, -6.66)
Initial guess of angles $\boldsymbol{\theta_i} = [\frac{-\pi}{12} \quad \frac{-\pi}{12}]$	
Calculated tip coordinates $\hat{\boldsymbol{x}}$ using θ=$\begin{bmatrix} l_1 cos(\theta_1) + l_2 cos(\theta_1+\theta_2) \\ l_1 sin(\theta_1) + l_2 sin(\theta_1+\theta_2) \end{bmatrix}$	
Calculate Jacobian $\boldsymbol{J} = \begin{bmatrix} \frac{\partial x_2}{\partial \theta_1} & \frac{\partial x_2}{\partial \theta_2} \\ \frac{\partial y_2}{\partial \theta_1} & \frac{\partial y_2}{\partial \theta_2} \end{bmatrix} = \begin{bmatrix} -l_1 sin(\theta_1) - l_2 sin(\theta_1+\theta_2) & -l_2 \sin(\theta_1+\theta_2) \\ l_1 cos(\theta_1) + l_2 cos(\theta_1+\theta_2) & l_2 \cos(\theta_1+\theta_2) \end{bmatrix}$	
Iterate θ in increments of j till absolute error ≤ set tolerance, $\Delta_j = \left|\boldsymbol{x} - \hat{\boldsymbol{x}}_{\boldsymbol{j}}\right| \le 0.05$ $\boldsymbol{\theta}^{\boldsymbol{j}+\mathbf{1}} = \boldsymbol{\theta}^{\boldsymbol{j}} + \boldsymbol{J}^{-\mathbf{1}}\Delta_j$	

$\theta = \begin{bmatrix}-30°\\-45°\end{bmatrix}$ is achieved in 8 iterations	$\theta = \begin{bmatrix}-30°\\-40°\end{bmatrix}$ is achieved in 8 iterations

The DH parameters corresponding to the initial and final configurations required for trajectory plotting though FK are listed in Table 1 and Table 2.

Table 2. Parameters of the initial leg position obtained through inverse kinematic analysis

	DH parameters						Resultant strain $\Delta l \angle \theta_R$	
	θ_1^i	θ_2^i	θ_3^i	l_0(mm)	l_1(mm)	l_2(mm)	l_3(mm)	
Adducting leg	-30°	-45°	- -	10.00	4.25	6.83	--	0.843 ∠52.5°
Abducting leg	-30°	-40°	-86°	10.00	4.35	4.77	5.11	1.135∠67.5°

Table 3. Parameters of the final leg position

	θ_1^f	θ_2^f	θ_3^f	Stroke at leg tip (mm)	
				$\Delta x = x_f - x_i$	$\Delta y = y_f - y_i$
Adducting leg	-42°	-45°	-	-1.90	0.93
Abducting leg	-15°	-38°	-86°	2.87	-0.07

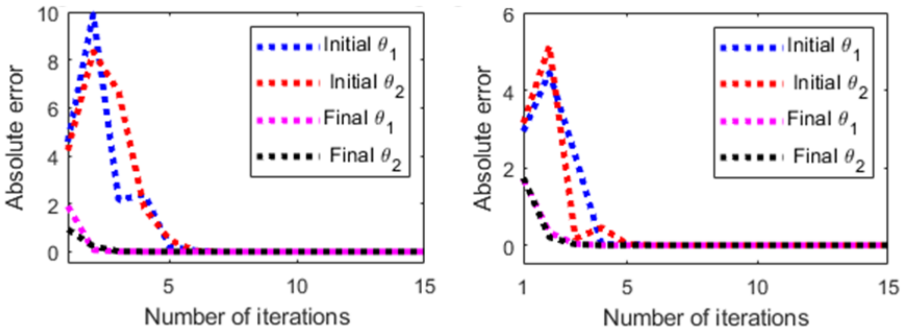

Fig. 8. (a) Convergence of 2R inverse kinematics (b) Convergence of 3R inverse kinematics

Convergence

4 Control

The Octabot has a total of DoF, two revolute DoF per leg. At a given time, two legs (four DoFs) are simultaneously controlled through one channel. There are a total of four channels that are programmatically switched on to obtain a sideways reciprocating gait. A set of the adducting legs on left side (Channel ADL) and the counterpart abducting legs (Channel ABR) on the right side are switched sequentially for movement in one-direction (left to right). The remaining set of legs (Channel ADR and Channel ABL) similarly contribute to motion in the opposite direction (right to left). All the legs are connected to a common ground terminal. The length of the NiTiNOL wire used for each of the abducting and adducting legs is 75 mm and 57 mm. The electrical resistance in Channel ADL & Channel ADR is 5Ω and in Channel ABL and Channel ABR is 6Ω. The wires are joule-heated at these voltages for 0.7s to achieve the transformation induced actuation of the legs. The heating (0.7s) and cooling time (1s) [6] of the wire determines the time period of each channel. A delay of 0.15s is maintained between the pulses of the subsequent channels to supplement the movement with inertial forces resulting from actuation, failing which, substantial slippage is observed. The overall operating frequency of the Octabot is 1.2 Hz. The pulse time-history of the four channels is shown in Fig.9.

An Arduino Uno microcontroller board has been programmed to generate analog pulsed signals to switch the channels as per the mentioned time sequence. The Channels are connected to the LN298N motor driver that serves as a four-channel power switching circuit. A regulated DC power supply provides the power input (5V, 0.8A) to the driver, while the pulses from the analog pins of the microcontroller are connected to the switch inputs. The switch outputs are connected to the respective channels to drive the actuators. A schematic layout of the electronic circuit is shown in Fig.10. For the demonstrating the reciprocating locomotion capability, the duration of each side-crawl is set to 10s.

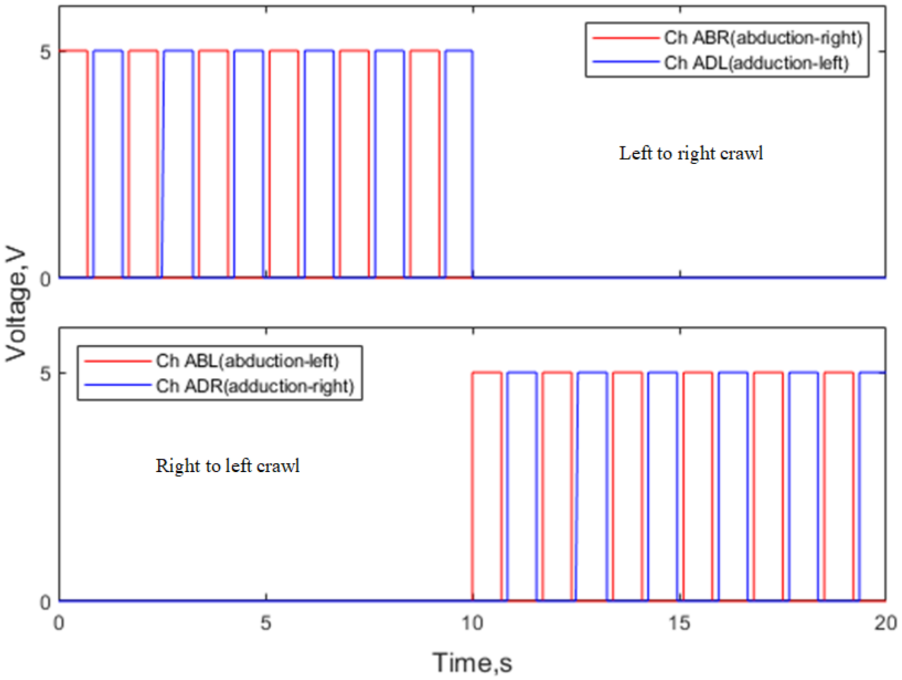

Fig. 9. Time-history of pulsed signal input

5 Results and discussions

The results of the kinematic analysis implemented in MATLAB are presented below. The computed initial and final positions of the adducting and abducting legs and the traced trajectory are depicted in Fig.11 and Fig.12. The initially set joint angles of the adducting leg calculated through IK for a random point (5.45, -8.70) in the workspace chosen as the tip coordinates are (-30°,-45°). The initially set angles for a chosen tip point (0.70, -8.70) for the abducting leg are (-30°,-40°,-86°). The final joint angles after actuation have been computed to be (-42°,-45°) and (-15°,-38°,-86°) respectively. The horizontal tip stroke during the complementing adducting and abducting legs are 1.90mm and 2.87mm. The computed change in CG position during each side-movement has been plotted in Fig.13.

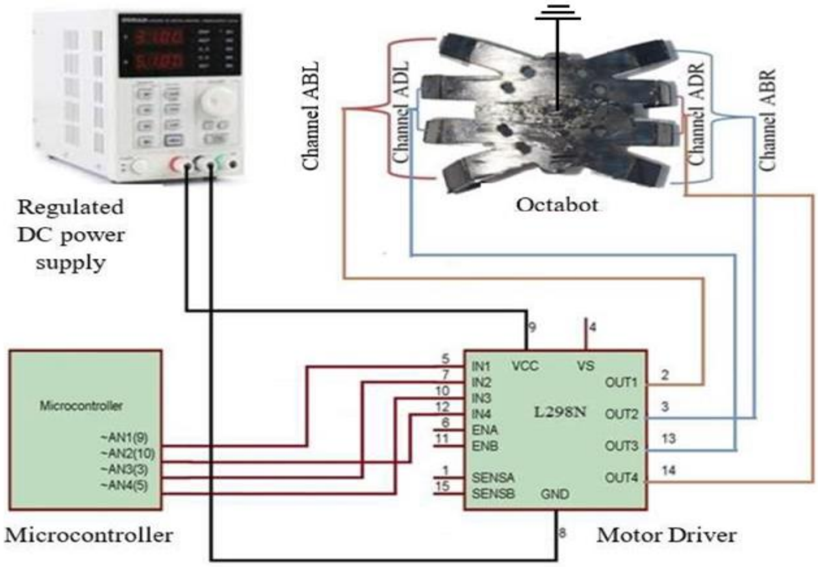

Fig. 10. Electronic circuit diagram

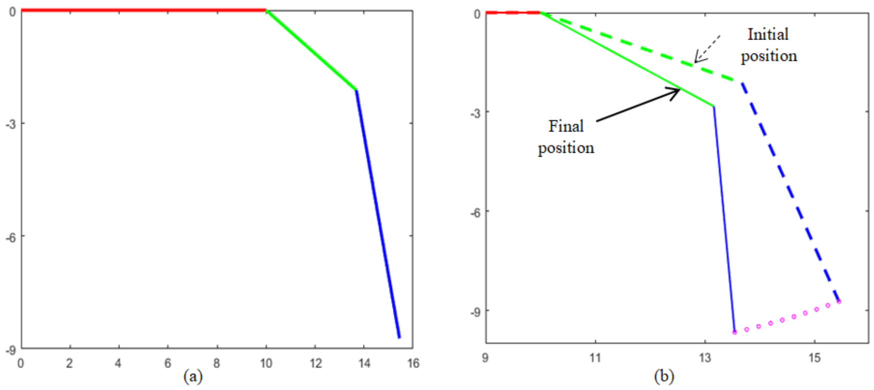

Fig. 11. (a) Configuration of the adducting leg (b) initial and final positions of the adducting leg

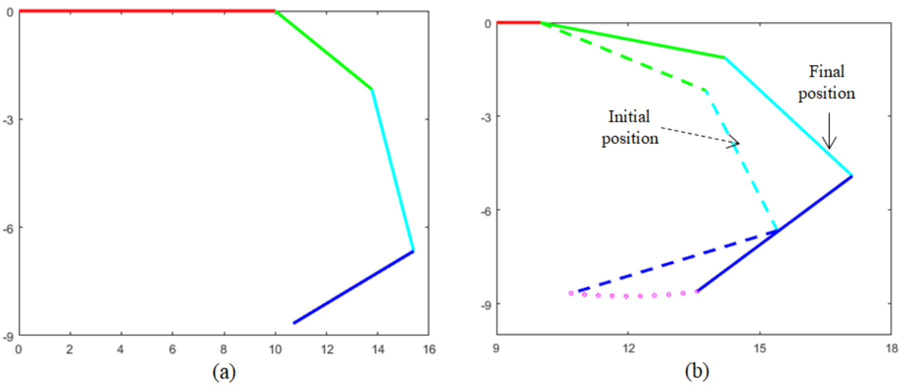

Fig. 12. (a) Configuration of the abducting leg (b) Initial and final positions of the abducting leg.

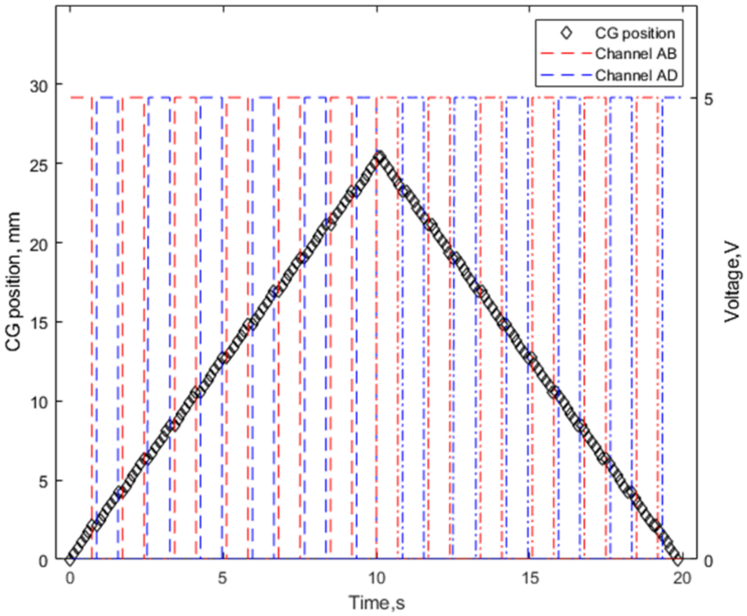

Fig. 13. Computed change in CG position

Electro-actuation tests have been performed on the Octabot prototype as detailed in Section 4. The measured values of the horizontal tip strokes are 2mm and 2.5mm in the adducting and abducting legs. The vertical stroke was observed to be insignificant, as per intended design. The crawling speed of the prototype was measured to be 2.5 mm/s, being in good agreement with the simulation results.

6 Conclusions and future work

The design and demonstration of a NiTiNOL actuated crab-like sideways crawling robot has been carried out in the present work. The design optimized by inverse and forward kinematic analysis has been fabricated using carbon fiber composite body employing flexure hinges for adduction and abduction of legs. The Octabot has successfully demonstrated the capability of a bidirectional side crawling gait at 2.5 mm/s in computation and experiments. Further work on the prototype will include an onboard electronic circuit and battery for untethered operation. Additionally, studies of crawling on uneven and inclined surfaces will be explored making necessary modifications to the design.

7 Acknowledgements

The authors express their gratitude to Dr. R. Ramakrishnan, Director, DRDO Young Scientists' Laboratory for Smart Materials for his valuable suggestions and encouragement in undertaking the present work.

8 References

1. Y. Chen, J. E. Grezmak, N. M. Graf, and K. A. Daltorio, "Sideways crab-walking is faster and more efficient than forward walking for a hexapod robot," Bioinspir Biomim, vol. 17, no. 4, Jul. 2022, doi: 10.1088/1748-3190/ac6847.
2. A. T. Baisch and R. J. Wood, "Design and Fabrication of the Harvard Ambulatory Micro-Robot."
3. R. S. F. Aaron M. Hoover, Robotics and Automation, 2008, ICRA 2008, IEEE International Conference on : date, 19-23 May, 2008. IEEE Xplore, 2008.
4. M. Soreni-Harari, R. St. Pierre, C. McCue, K. Moreno, and S. Bergbreiter, "Multimaterial 3D Printing for Microrobotic Mechanisms," Soft Robot, vol. 7, no. 1, pp. 59–67, Feb. 2020, doi: 10.1089/soro.2018.0147.
5. R. J. Wood, S. Avadhanula, R. Sahai, E. Steltz, and R. S. Fearing, "Microrobot design using fiber reinforced composites," Journal of Mechanical Design, Transactions of the ASME, vol. 130, no. 5, May 2008, doi: 10.1115/1.2885509.
6. "NICKEL-TITANIUM ALLOY PHYSICAL PROPERTIES." [Online]. Available: http://www.dynalloy.com
7. Howell LL. Compliant mechanism. New York: John Wiley & Sons, 2001
8. Y. Q. Yu, Q. Li, and Q. P. Xu, "Pseudo-rigid-body dynamic modeling and analysis of compliant mechanisms," Proc Inst Mech Eng C J Mech Eng Sci, vol. 232, no. 9, pp. 1665–1678, May 2018, doi: 10.1177/0954406217707547.
9. H. J. Su, "A pseudorigid-body 3r model for determining large deflection of cantilever beams subject to tip loads," J Mech Robot, vol. 1, no. 2, 2009, doi: 10.1115/1.3046148.